21. CRACK GROWTH IN CONSTANT LOAD AND CONSTANT DISPLACEMENT CYCLING

by

J. C. Radon, P. M. S. T. de Castro and L. E. Culver

Department of Mechanical Engineering
Imperial College of Science and Technology
Imperial College, London SW7 2BX

SUMMARY

Fatigue tests were performed on two materials, a mild steel BS15 and a high strength Al-alloy RR58, using Double Cantilever Beam specimens in air at 21°C, and certain aspects of fatigue crack growth were studied.

The results from steel were analysed using a newly proposed crack growth law which is particularly useful in design applications. This law has a form:

$$\frac{da}{dN} = A \left(\frac{\lambda - \lambda_{th}}{K_c^2 - K_{max}^2}\right)^{\alpha}$$

where $\lambda = K_{max}^2 - K_{min}^2 = 2 \Delta K K_m$, and represents the crack growth in a linear fashion on a log/log scale. Further, a transient crack growth retardation was illustrated for a high-low loading sequence, and finally a comparison of crack growth at two widely different frequencies (0.1 Hz and 35 Hz) indicated only a slight increase for slow speed cycling in Region II.

Constant load and constant displacement cycling tests were performed on RR58 at 0.1 Hz. Crack growth rates were basically identical for both types of cycling, thus confirming that the methods are equivalent. However, some additional tests at 35 Hz suggested substantial differences in the crack growth rate, contrary to the results on mild steel.

1. Introduction

1.1 GENERAL

A great deal of research effort has recently been directed towards the investigation of the crack propagation stage of the fatigue process. The description of the stress field close to the tip of a crack using the concept of a stress intensity factor, K, presented a suitable conceptual framework for the detailed investigation of the fatigue crack growth process as well as for other subcritical crack propagation situations, such as static stress corrosion cracking, corrosion fatigue and creep cracking. While the static and environmental problems are discussed elsewhere |1| this paper deals exclusively with the cylic crack growth. In particular, two specific types of cycling are considered: the first, performed at constant load is compared with the second at constant load point displacement. Both types, as described here, are essentially elastic deformations with the crack propagating through an elastic field; a plastic zone enveloping the actual tip of the crack is considered to be small in comparison to the crack length. It is known that the fatigue process is one of the most frequently encountered types of damage to engineering structures and both types of cycling are very common, the constant displacement cycling probably being predominant.

1.2. FATIGUE CRACK GROWTH

The basic formulation of the fatigue crack propagation process is due to Paris, |2|

$$\frac{da}{dN} = C\ (\Delta K)^m \qquad (1)$$

where a is the crack length, N is the number of cycles, and C and m are constants. Numerous empirical forms of cyclic crack propagation relationships

derived basically from Eq. 1. have been proposed |1|. They are helpful for a realistic assessment of fatigue life of many engineering structures. As it is known, inherent defects in structural materials drastically reduce the period of crack initiation. Consequently the total fatigue life consists substantially of crack propagation. The effect of the principal parameter ΔK, Eq. 1. on the crack growth rate has been recognized for some time, but the influence of other factors was considered only recently.

For metals it was originally suggested |2| that K_m was of minor importance when compared with ΔK, but more recently attention has been drawn to the importance of K_m on the rate of fatigue crack propagation. In particular, in the early tests on round bars of carbon steel it was found that mean stress cannot be discarded as having only a secondary influence on crack growth |3|. Similar conclusions have been drawn for some Al-alloys |4|. Other rather unexpected results have been reported on a range of polymers |5| and the behaviour of polycarbonate may indicate a complicated influence of K_m on crack growth. When the effects of loading frequency were investigated on thick centrally notched polycarbonate plates, it was found that a transition point in the value of $\dot{K}$ (= dK/dt) term existed, above and below which the mean stress intensity and frequency effects were different. Above this critical value (4000 psi$\sqrt{i}$ s^{-1}) the K_m effect was small; below that K_m had a significant effect on da/dN under the same applied K_{max} and K_{min}.

Contrary to the empirical approach |2|, Radon |6| considered plastic strains at the boundary of the deformed zone of radius r which can be expressed as:

$$\epsilon = \gamma_y \frac{2r \cos \phi}{d} \qquad (2)$$

where d and ϕ are polar co-ordinates measured from the crack tip and γ_y is the shear strain at the elasto-plastic boundary. Using the Manson-Coffin relation for a relatively small plastically deformed zone, the cyclic life N can be expressed:

$$N = \frac{Const}{\epsilon^2} \qquad (3)$$

and consequently

$$N = \frac{Const}{(2r)^2} \qquad (4)$$

and the rate of crack propagation is then

$$da/dN = Const.\ K^4 \qquad (5)$$

Following these considerations Arad |7| reformulated Eq. 5. to

$$da/dN = \beta(\lambda)^n \tag{6}$$

where β is a constant and λ equals $(K^2_{max} - K^2_{min})$ which for $K_{min} = 0$ simplifies to Eq. 1. Recognizing the importance of K_m described above, Arad pointed out that the influence of K_m is, in fact, in

$$\lambda = 2\ \Delta K.K_m \tag{7}$$

It may be also noted that

$$\lambda = (1 - R^2)\ K^2_{max} \tag{8}$$

thus

$$da/dN = \beta\lambda^n = \beta(1 - R^2)^n\ (K^2_{max})^n \tag{9}$$

Since in most practical cases σ_{max} and σ_{min} are constants associated with the characteristics of the external disturbance, the growth of the crack will not change the value of R even though the value of K_{min} and K_{max} parameters increases gradually. Thus in the above equations $(1 - R^2)$ is a constant and hence a plot of da/dN against λ can be changed to a plot of da/dN against K_{max} with β replaced by $\beta\ (1 - R^2)^n$.

Using the formulation of Eq. 6., the influence of the mean stress intensity K_m was studied on a range of high strength Al-alloys; it was concluded that in general they are, apparently, highly sensitive to K_m |7,8|. However, in steels the degree of sensitivity to K_m was not so distinct and some controversial results may be found in the literature, a clear explanation being not yet available. It seems at present that crack propagation in high strength steels is not only K_m sensitive, but also depends on the ultimate K_c value and the threshold |9|.

Arad's law has been recently modified by Branco |10| to cover the full range of the observed fatigue crack propagation behaviour, from a very low threshold (Region I cf. for example Fig. 10) to very high values of ΔK, (Region III) in the following form:

$$\frac{da}{dN} = A\left(\frac{\lambda - \lambda_{th}}{K_c^2 - K^2_{max}}\right) = A\phi^{\alpha} \tag{10}$$

where

$$\lambda = K^2_{max} - K^2_{min} = 2\Delta K.K_m \tag{11}$$

A and α are constants, λ_{th} represents the threshold value of λ for crack propagation, and K_m is the mean value of the stress intensity factor. A detailed discussion of the application of Eq. 10. for a range of metals may be found in |8|. Recently it has been successfully used by Sutton |11| for the analysis of the crack growth in an epoxy resin.

It will be realised that the transition between Regions I and III, commonly described as Region II, is usually well characterised by the Paris law, equation (1). However, the extension of Eq. 1. to Region I invariably leads to an overestimate of the crack growth, whereas in Region III the growth will be underestimated. Except for special conditions of low cycle fatigue which are not the subject of the present work, a substantial fast crack growth in this region (III) is experienced in real engineering situations only very infrequently.

On the other hand, a very slow growth in Region I, often close to the threshold region, is commonly encountered in many technical applications and its importance in engineering design cannot be adequately stressed. The long-life situation in Region I will be discussed in detail later.

One aspect of fatigue studies which has been of interest concerns the influence of the testing method, as illustrated by the low cycle fatigue studies carried out under load or strain control using uncracked specimens |12|, or, more recently, fracture mechanics specimens |13,14|. Another aspect of fatigue also recently investigated concerns the influence of the sequence of different load amplitudes on the fatigue crack propagation behaviour, namely the phenomenon of crack growth retardation when loading cycles of a given ΔK are followed by cycles of a relatively lower ΔK.

The present paper reports work undertaken to obtain further evidence on the applicability of the law expressed by equation (10) to the fatigue crack propagation process of mild steel BS15, by performing tests at a lower frequency than those used in previous investigations, |9|, in order to assess the possible frequency effect.

The paper also reports on a crack propagation study of aluminium alloy RR58 under constant load and constant displacement cycling. The constant displacement tests reproduce a loading situation frequently found in engineering practice, and therefore the current work examines the possibility of applying conventional fatigue crack propagation data obtained under conditions of constant ΔK loading to this situation. A typical example of a displacement controlled fatigue condition is constrained structural elements subjected to varying temperature or loading.

2. Experimental

2.1. MATERIALS

Mild steel BS15 is a 0.19% carbon steel commonly used in welded structures. It was supplied in rolled plates 11.2 mm thick.

The aluminium alloy RR58 is a precipitation hardenable Al-Cu-Mg alloy widely used in the aeronautical industry, in particular in the supersonic aircraft Concorde. The material was supplied in plates 914 x 914 x 76 mm, strained 2.25% after solution heat treatment at 530°C followed by water quenching.

The composition and mechanical properties of both materials may be found in Table 1.

2.2 SPECIMENS

The most frequently used Fracture Mechanics specimens, such as the three point bend or compact tension specimens, produce an increasing value of stress intensity factor K with increasing crack length, assuming the load P is kept constant. It is possible, however, to design a specimen such that its compliance C is a linear function of crack length, thus giving a constant value of K at constant P irrespective of crack length, as shown by the equation

$$K = P \sqrt{\frac{E}{2B_n(1-\nu^2)} \frac{dC}{da}} \qquad (12)$$

where E is Young's modulus, ν Poisson's ratio and B_n the net fracture width. This type of specimen, known as the contoured double cantilever beam (DCB), is

described in detail in |15|. In order to comply with the condition of dC/da = constant, a contoured shape was chosen having the form

$$\frac{3a^2}{h^3} + \frac{1}{h} = 38 \qquad (13)$$

where h is the specimen height at a crack length a.

All the specimens used had the same overall dimensions, Figure 1, and were provided with grooves on both sides in order to increase constraint, to ensure plane strain conditions, and also to maintain the desired path of the crack along the specimen middle plane.

The mild steel BS15 specimens, of 11.2 mm gross thickness (the plate thickness) were orientated to ensure crack growth along the rolling direction. Grooves 3.5 mm deep were machined on both sides, and a slot approximately 40 mm long was cut. The slot was extended into a swallow tail front and subsequently indented with a razor blade to form a sharp crack starter.

Aluminium alloy RR58 specimens had 9.5 mm gross thickness, and were provided with 0.75 mm deep grooves on both sides. The specimens were cut from the plate in such a way that the crack propagated along the rolling direction whilst the load was applied in the short transverse direction. Each specimen was aged in a salt bath at 190°C for 30 hours, to give a hardness in the range 145-150 VPN and a slot was prepared as described for BS15 specimens.

2.3 TESTING PROCEDURE

The stress intensity factor calibration of BS15 and RR58 specimens was obtained experimentally by determining the slope of the compliance versus crack length (dC/da) plot for each specimen, and using equation (12). It is to be noted that once dC/da is known, a linear relationship is established between K and applied load P.

The critical value of the stress intensity factor K_c may be obtained, provided unstable crack propagation occurs under linear elastic conditions. For RR58 specimens, this condition was fulfilled; therefore, experimental compliance calibration and calculation of K_c were performed by precracking under monotonic loading, in the Instron TT-C machine (45kN load capacity). All tests were conducted in laboratory air and at room temperature. The

crack was extended by about 25 mm, using a constant crosshead speed of 1.3 mm/min. Jaw separation and load were recorded automatically, and the crack length observed with a travelling microscope giving 10x amplification and reading to 0.01 mm.

However, in the case of the steel it was found that the crack growth only occured after gross plastic deformation thus K_c values could not be established following the technique described for RR58 specimens. Therefore the stress intensity factor calibration had to be carried out during the fatigue test. The calibration was performed using the Instron machine, measuring the compliance for a range of crack length values corresponding to different stages of the fatigue crack growth.

In the fatigue test programme, it was desired to obtain results for specific K_m and ΔK values. The settings of the load limits in the fatigue machines used here (a hydraulic Denison T42C2 of 100 kN load capacity and a hydraulic Avery of 500 kN load capacity) were made taking into account equation (12), and remembering that for the DCB specimens used, dC/da is constant. Therefore, for an appropriate value of load P

$$K = C_1 P \tag{14}$$

where C_1 is a constant, and to obtain a given $(K_{max} - K_{min}) = \Delta K$ range it was only necessary to set the following limits in the fatigue machine:

$$P_{max} = K_{max}/C_1 \tag{15}$$

and

$$P_{min} = K_{min}/C_1 \tag{16}$$

Hence, any repetitive loading pattern of constant amplitude produced a cyclic variation of K, the limits of which were also constant, as the crack extended. Crack growth was monitored using the travelling microscope as previously described.

3. Results and Discussion

3.1. COMPLIANCE CALIBRATION; CALCULATION OF ALUMINIUM ALLOY RR58 FRACTURE TOUGHNESS K_c

As pointed out above, it was found that unstable crack propagation was obtained for aluminium alloy RR58 under linear elastic conditions, Figure 2. Therefore it was possible, from a single monotonic loading of each specimen, during which the crack extended for about 25 mm, to obtain not only the complinace calibration, but also the value of K_c.

The specimen was loaded monotonically at a constant crosshead speed of 1.3 mm/min. On reaching a maximum load the crack suddenly jumped and the load decreased to a constant value, Figure 2. The value of the maximum load was found to be related to the sharpness of the crack starter; it was increased with the bluntness of the starter.

While using the same crosshead speed, it was observed that the crack subsequently propagated under substantially constant critical load P_c. A typical record of the complete load versus deflection curve is presented in Figure 2. The compliance calibration was obtained from readings of crack length, taken with a microscope, during the monotonic loading of the specimen. The compliance calibration for one of the specimens tested is presented in Figure 3. The linear variation of compliance with crack length appears clearly, thus confirming experimentally that this form of DCB specimen satisfies the relation dC/da = constant.

K_c was obtained by substituting the cracking load, P_c, into equation (12). In the present fracture toughness tests K_c ranged from 20.6 to 22.7 $MN/m^{3/2}$, as can be observed in Table 2, where the critical loads and dC/da for the different specimens are also recorded. It will be realised that specimens with higher cracking loads have lower dC/da values, thus maintaining the fracture toughness values nearly constant.

These results may be compared with values ranging from 20.7 to 23.9 $MN/m^{3/2}$, [8], previously obtained following the same procedure but at a different crosshead speed (0.05 mm/min) and with the value of 22 $MN/m^{3/2}$, [16], obtained following the ASTM E399-72 method, using three-point bend specimens 19 mm thick. It is interesting to note that although using thinner specimens,

the present results are similar to those ASTM E399-72 valid K_{1c} results. This is explained by remembering that the side grooves in the specimens promote plane strain conditions at the crack tip. Considering the strain rates used in the present tests, it is suggested that K_c is mainly strain rate insensitive, thus following the trend reported for the aluminium alloy of comparable composition Alcan GB-B26S in |17|.

As regards mild steel BS15, it has already been said that due to plastic bending of the arms of the specimen, the standard method of K_c determination and compliance calibration was not possible. The calibration was carried out during the fatigue tests, simply measuring the compliance for different stages of crack propagation. A typical value of dC/da for BS15 specimens was $5.44 \times 10^{-6} N^{-1}$.

3.2. FATIGUE CRACK PROPAGATION IN MILD STEEL BS15 AT 0.1 Hz, LABORATORY AIR AND ROOM TEMPERATURE

The aim of this study was to obtain fatigue crack propagation data, under conditions of constant mean stress intensity factor and at 0.1 Hz frequency. In order to enable comparison with results previously obtained at 35 Hz |9|, a mean stress intensity factor of $K_m = 47.5$ MN/m$^{3/2}$ was selected.

The crack growth versus number of cycles curve obtained for two consecutive tests ($\Delta K = 31.6$ and $\Delta K = 12.6$ MN/m$^{3/2}$) is represented in Figure 4. A transient of crack growth retardation was observed before the steady, linear growth characteristic of the lower value of ΔK was attained. It will be noticed that fatigue testing using contoured DCB specimens allows a clear identification of retardation effects, since each value of da/dN is obtained after a suitable amount of crack growth under constant load range and therefore constant stress intensity range, as schematically represented in Figure 5a.

In Figure 6 the present results are plotted together with two curves of da/dN versus ΔK reported in |9|, one for the same K_m value but different frequency (35 Hz), and the other for $R = K_{min}/K_{max} = 0$ again at 35 Hz.

Comparing the present results for $K_m = 47.5$ MN/m$^{3/2}$ with the previous results for the same K_m, a reasonable agreement is found, since the maximum ratio between the present da/dN values, and those predicted in the curve for equal ΔK, is about 2, clearly within the usual scatter limits for this type of

test. Thus, although there is a slight increase in da/dN for low frequency cycling in Region II, the fatigue crack propagation behaviour of mild steel BS15 appears to be essentially frequency insensitive in the range 0.1 Hz to 35 Hz. The results of more recent, but not yet published tests performed at 0.25 Hz support the present observations, Figure 6. In Region I the crack growth rate decreases only slightly with a lower frequency and the consequent increase of the threshold level K_{th}. In Region II the crack propagation is slightly faster, while the results in Region III are practically identical for all frequencies investigated (from 0.1-35 Hz).

Considering now the results in Regions II, the inadequacy of the simple form of equation (1) is clear. The slope of Region II for R = 0 is markedly different from the slope of the same region for $K_m = 47.5$ MN/m$^{3/2}$, and this may be observed in Figure 6. The present results for the same value of K_m as well as a single result for R = 0 are plotted using equation (10) in Figure 7. The values of ΔK_{th} and K_c used here ($\Delta K_{th} = 3.2$ MN/m$^{3/2}$ and $K_c = 98.0$ MN/m$^{3/2}$) were obtained from |9|. For comparison, the scatterband of results, Ref. |9|, for R = 0, and for $K_m = 15.8$, 31.6 and 47.5 MN/m$^{3/2}$ is also presented in Figure 7. Equation (10) enables the representation of da/dN versus ΔK data in a linear fashion on a log/log scale, irrespective of the Region of crack propagation under consideration and of the value of R.

Finally, it should be mentioned that the fracture appearance was essentially plane, without evidence of any transition to single or double shear, thus implying that the tests were conducted under plane strain conditions.

3.3 FATIGUE CRACK PROPAGATION IN ALUMINIUM ALLOY RR58 AT 0.1 Hz LABORATORY AIR AND ROOM TEMPERATURE

Fatigue crack propagation studies in aluminium alloy RR58 found in the literature, |10|, are only concerned with load cycling. Constant displacement tests were carried out in order to compare the load cycling with constant load point displacement cycling situation, since the latter is frequently found in engineering practice. There is some evidence |12| showing that different material behaviour in load and strain cycling, as well as interaction effects in varying ΔK tests (such as retardation), may eventually lead to a different da/dN versus ΔK relation.

Load cycling results obtained in the preliminary tests are plotted in Figure 8, where the approximate scatterband of load cycling results |10|

is also included. A good agreement may be observed. Since the tests were conducted under R = O, Region II can be described by equation (1) with exponent m = 5.3. A higher value of m was not unexpected considering the fracture toughness of this material, since it has been shown that the value of m tends to increase for low levels of fracture toughness, |18|.

Constant load point displacement cycling results were obtained subsequently. The method consisted of conducting first a conventional load controlled test, which for this specimen geometry corresponded to constant ΔK cycling. After obtaining an adequate amount of data to characterize the crack growth behaviour at a particular value of ΔK, the testing programme was switched to displacement control. Therefore, the first cycles of this new type of fatigue loading were conducted under ΔK similar to that previously used, but, as the crack propagated, the load necessary to impose the same constant displacement began to decrease since the specimen was becoming more compliant. The load (or stress intensity factor) range during this constant displacement cycling test is schematically represented as in Figure 5b.

The initial value of ΔK for the constant displacement test was $\Delta K = 18.4\ MN/m^{3/2}$; this value was used for the previous load cycling test represented by the straight lines in Figure 9. The subsequent displacement controlled test is represented by the two curves in the same Figure. As anticipated, ΔK was decreasing during the test. A number of crack growth rates obtained by graphical differentiation, together with the corresponding values of ΔK are recorded in Figure 8.

It was found that the displacement cycling results follow closely the pattern of the load cycling data, since they fall well within the scatterband for load cycling tests, Figure 8. This suggests that the present continuous variation of ΔK does not induce any retardation effect, unlike that seen above for discontinuous high-low sequences (Figures 4 and 5a). On the other hand, crack growth occurred under macroscopically linear elastic conditions. This implies that the effects connected with the load or strain cycling behaviour in low cycle fatigue tests, such as cyclic creep, were not present.

The influence of frequency in the crack growth appears to be much stronger than that observed in steel (cf. Figure 6) although the characteristic behaviour is nearly the same, Figure 10. The tests so far performed for R = O indicated a decrease of the crack growth rate with

decreasing frequency in Region I, while at higher values of ΔK a reversal of this behaviour was recorded. When cycling at ΔK values above 6.5 $MN/m^{3/2}$ the crack propagated faster at low frequencies. This unexpected increase is probably connected with the increasing "static" slow growth at very low cyclic speeds and requires further investigation.

4. Conclusions

1) A fatigue crack propagation law recently proposed was used to analyse experimental results obtained from tests on contoured double cantilever beam specimens of mild steel BS15. This law, which represents the crack growth in a linear fashion on a log/log scale, was shown to be applicable to the present data. During these experiments it was possible to observe a transient phenomenon of retardation for high-low loading sequences. The work was conducted at a lower frequency than those used in previous investigations; it is concluded that this material is essentially frequency insensitive.

2) Fatigue crack propagation behaviour of aluminium alloy RR58 was studied using contoured double cantilever beam specimens subjected to constant load and constant load point displacement cycling. An essentially similar behaviour was observed for these two different testing conditions, i.e. da/dN was found to be determined by ΔK irrespective of testing method. It is suggested that retardation effects are not displayed in continuously decreasing ΔK situations, unlike those observed in discontinuous high-low sequences.

3) In the constant load and constant displacement cycling tests no difference in crack growth behaviour should be expected on the grounds of a comparison with conventional low cycle fatigue studies (where such differences occur), since the present fatigue tests are conducted under linear elastic conditions.

4) A well defined frequency sensitivity was observed for the tests performed on Al-alloy RR58, the crack propagation rate increasing with decreasing frequency for $\Delta K > 6.5\ MN/m^{3/2}$. This behaviour was reversed for $\Delta K < 6.5\ MN/m^{3/2}$.

References

1) "Fracture - an advanced treatise", Ed. H. Liebowitz, Academic Press 1972.

2) Paris, P. C., "The fracture mechanics approach to fracture", Proc. 10th Sagamore Army Mat. Res. Conf., Syracuse University, 1964, p 107.

3) Nakazawa, H., Koizumi, T., Honma, H. and Sayanaghi, H., "The effect of mean stress on fatigue crack initiation and propagation", Bull. Jap. Soc. Mech. Eng. 1969, 12, 53, p 958.

4) Pearson, S., "The effect of mean stress on fatigue crack propagation in half inch thick specimens of aluminium alloys of high and low fracture toughness", RAE, TR. 68297, 1968.

5) Arad, S., Radon, J. C. and Culver, L. E., "Design against fatigue failure in thermoplastics", Eng. Fract. Mech., 4 , p 511-522, 1972.

6) Radon, J. C., "Low endurance fatigue of cast irons and cast steels", Ph.D. thesis, University of London, 1966.

7) Arad, S., "Fracture Mechanics analysis of fatigue crack growth in viscoelastic solids", Ph.D. thesis, University of London, 1972.

8) Branco, C. M., "Fracture mechanics approach to environmental and elastic plastic fatigue crack propagation", Ph.D. thesis, Imperial College, University of London, 1976.

9) Branco, C. M., Radon, J. C. and Culver, L. E., "Growth of fatigue cracks in steels", Metal Science, 1976, p 149.

10) Branco, C. M., Radon, J. C. and Culver, L. E., "Influence of mean stress intensity on fatigue crack growth in an aluminium alloy", J. Mech. Eng. Sci., 17, (4), 1975, p 199.

11) Sutton, S. A., Eng. Fract. Mech., 6. 1974, p 587.

References (continued)

12) Radon, J. C. and Oldroyd, P. W. J., "Creep of irons and steels in uniaxial load cycling", Proc. II Int. Conf. Mech. Behavior of Materials, ICM, Boston, 1976, p 752-758.

13) Branco, C. M., Radon, J. C. and Culver, L. E., "Elastic-plastic fatigue crack growth under load cycling", J. Strain Analysis, 12, (2), 1977, p 71.

14) Radon, J. C., Branco, C. M. and Culver, L. E., "Creep in low endurance fatigue of mild steel", Int, J. Fracture, 13, (5), 1977, p 595.

15) Radon, J. C., Johnson, F. A. and Turner, C. E., "Use of the double cantilever beam test in fracture studies", in: Practical Applications of Fract. Mech. to Pressure Vessel Techn., I. Mech. E., 1971, p 48.

16) Matthews, W. T., "Typical plane strain fracture toughness of aircraft materials", in: AGARD-AG-176, 1974, p 509.

17) Johnson, F. A. and Radon, J. C., "Mechanical and metallurgical aspects of fracture behaviour of an Al-alloy", Int, J. Fract. Mech., 8, (1), 1972, p 21.

18) Youssefi, K., "Fatigue crack initiation and propagation in steels exposed to inert and corrosive environments", Ph.D. thesis, University of California, Berkeley, 1978.

TABLE 1

COMPOSITION AND MECHANICAL PROPERTIES OF ALUMINIUM ALLOY RR58

Element	Cu	Mg	Mn	Si	Fe	Ti	Zn	Ni
Weight %	2.64	1.65	0.03	0.23	1.15	0.06	0.06	0.10

Young's Modulus, E = 75 GN/m^2

Poisson's Ratio, ν = 0.33

Ultimate tensile stress, σ_{uts} = 450 MN/m^2

0.1% Proof stress, σ_y = 367 MN/m^2

Minimum elongation, ε_r = 6%

COMPOSITION AND MECHANICAL PROPERTIES OF MILD STEEL BS15

Element	C	Mn	Si	P	Ni	Cr	Mo	Nb
Weight %	0.19	0.59	0.028	0.021	0.02	0.01	0.02	0.005

Young's Modulus, E = 207 GN/m^2

Poisson's Ratio, ν = 0.3

Ultimate tensile stress, σ_{uts} = 585 MN/m^2

0.1% Proof stress, σ_y = 401 MN/m^2

Minimum elongation, ε_r = 28%

TABLE 2

K_{1c} VALUES OF ALUMINIUM ALLOY RR58 SPECIMENS

Spec	P_c (N)	dC/dn (N^{-1})	K_{1c} ($MN\ m^{-3/2}$)
C75	2158	2.00×10^{-5}	22.7
C77	2002	2.14×10^{-5}	21.8
C81	1735	2.54×10^{-5}	20.6
C85	1846	2.34×10^{-5}	21.0

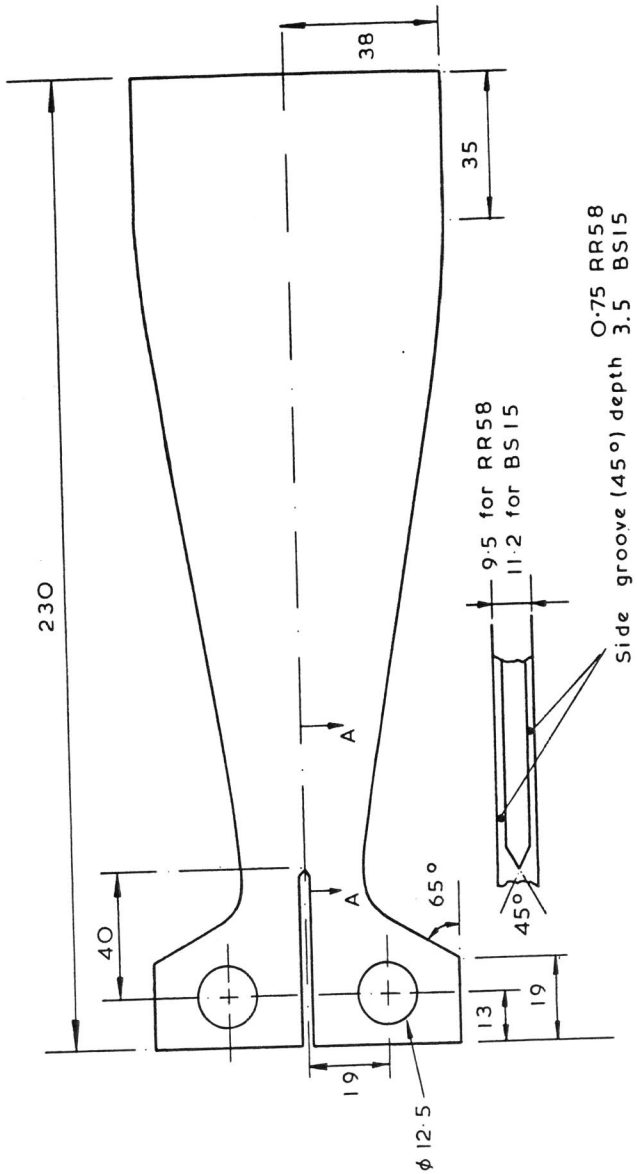

Figure 1: Contoured double cantilever beam specimen

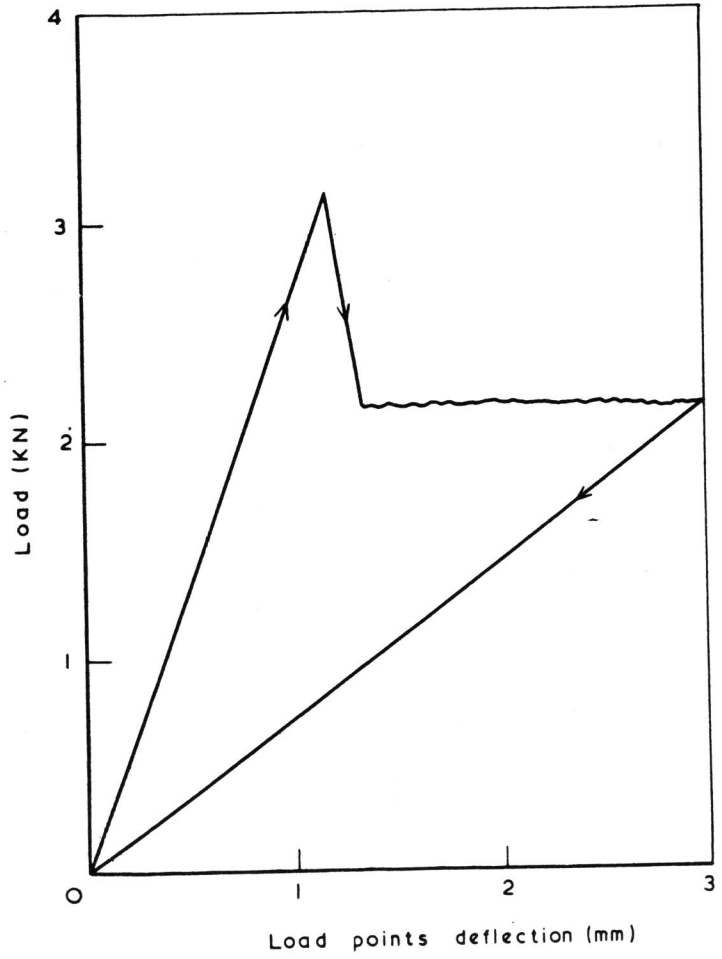

Figure 2: RR58. Typical load versus load points deflection record. 9.5 mm thick DCB specimen.

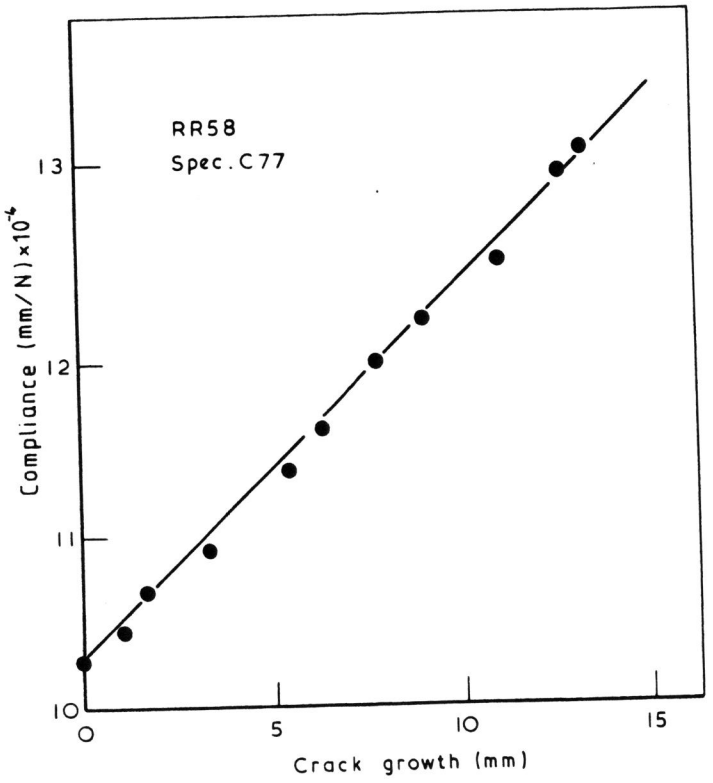

Figure 3: Al-Alloy RR58. Typical compliance versus crack growth curve. 9.5 mm thick specimen.

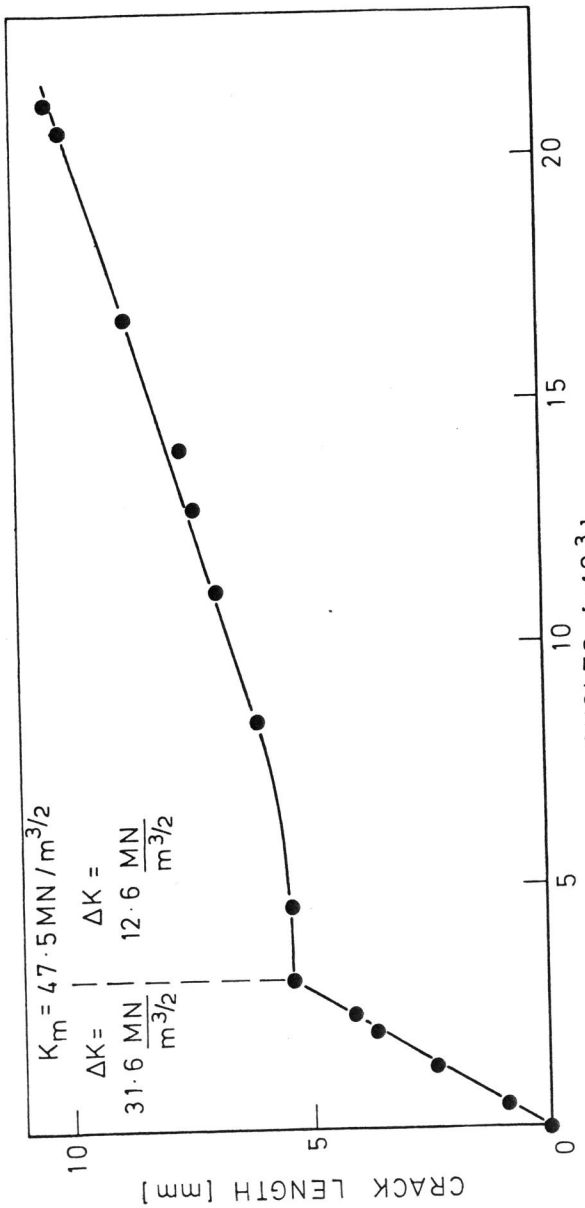

Figure 4: Crack growth pattern for two different and consecutive values of ΔK. Mild steel BS15, laboratory air, 0.1 Hz

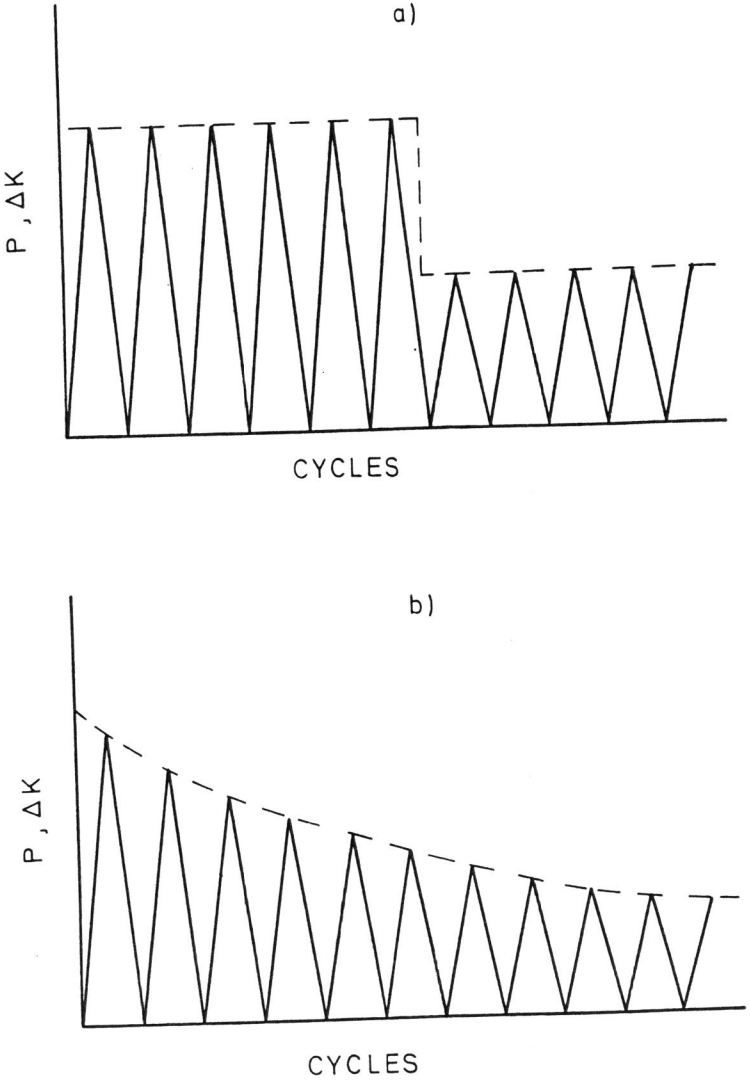

Figure 5: Fatigue testing using DCB specimens, $R = 0$. Schematic
(a) load cycling
(b) displacement cycling

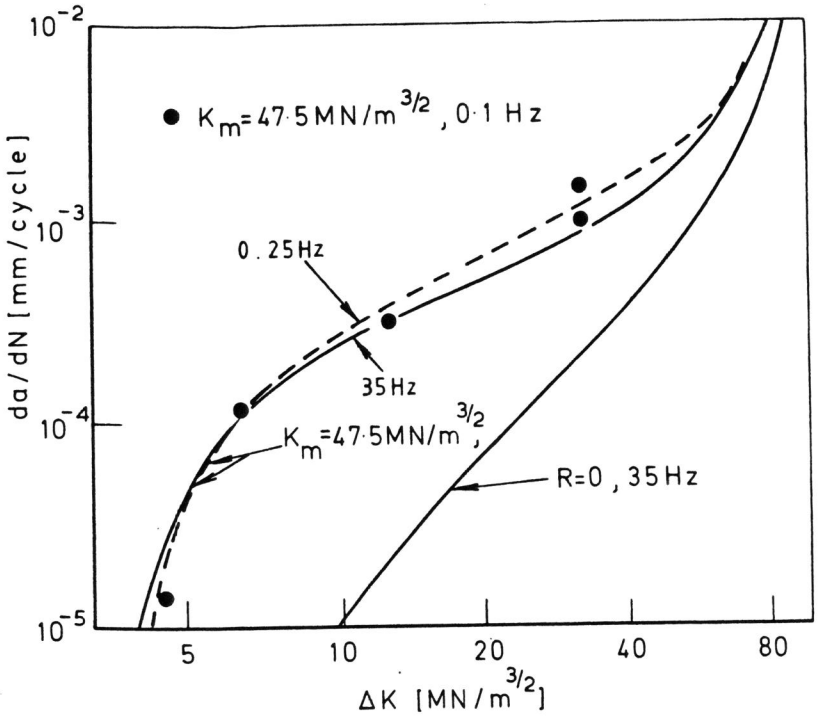

Figure 6: BS15: Crack growth rate versus ΔK

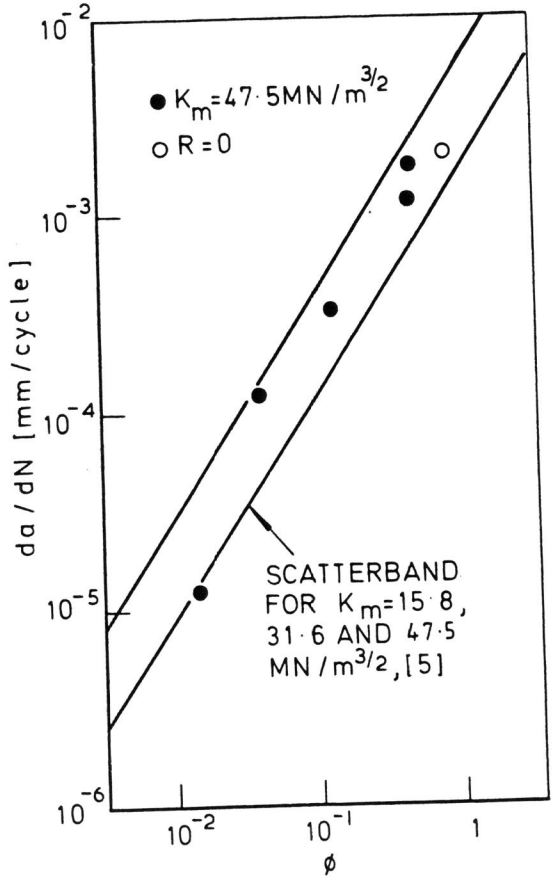

Figure 7: BS15: Crack growth rate versus ϕ (equation 2), 0.1 Hz

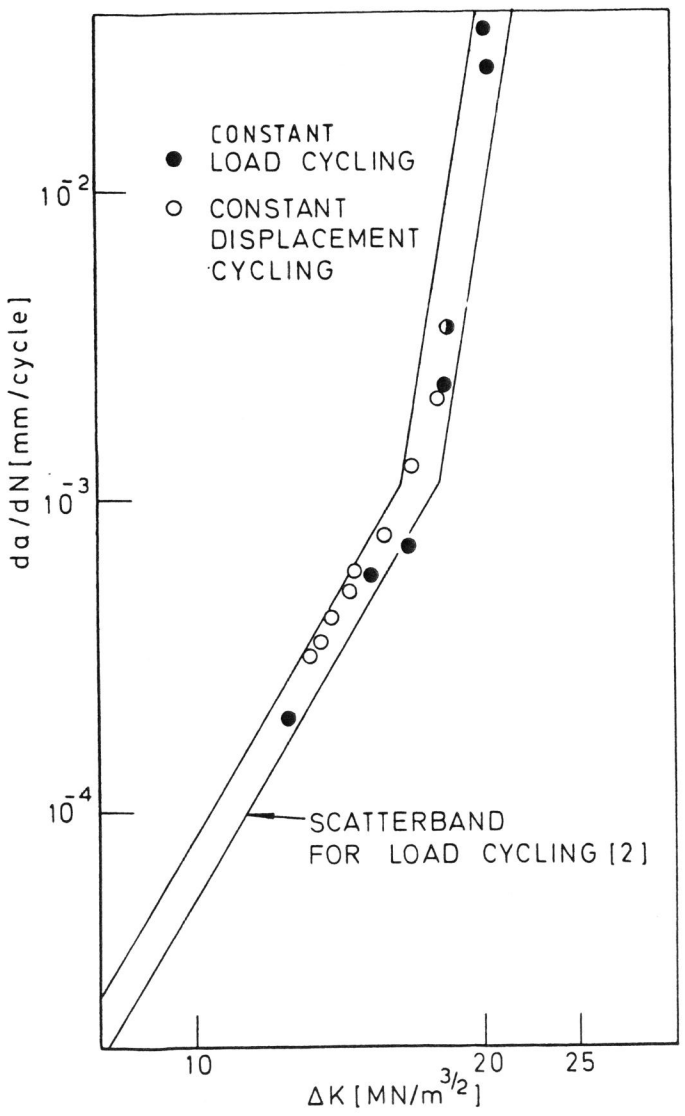

Figure 8: RR58: Crack growth rate versus ΔK, 0.1 Hz

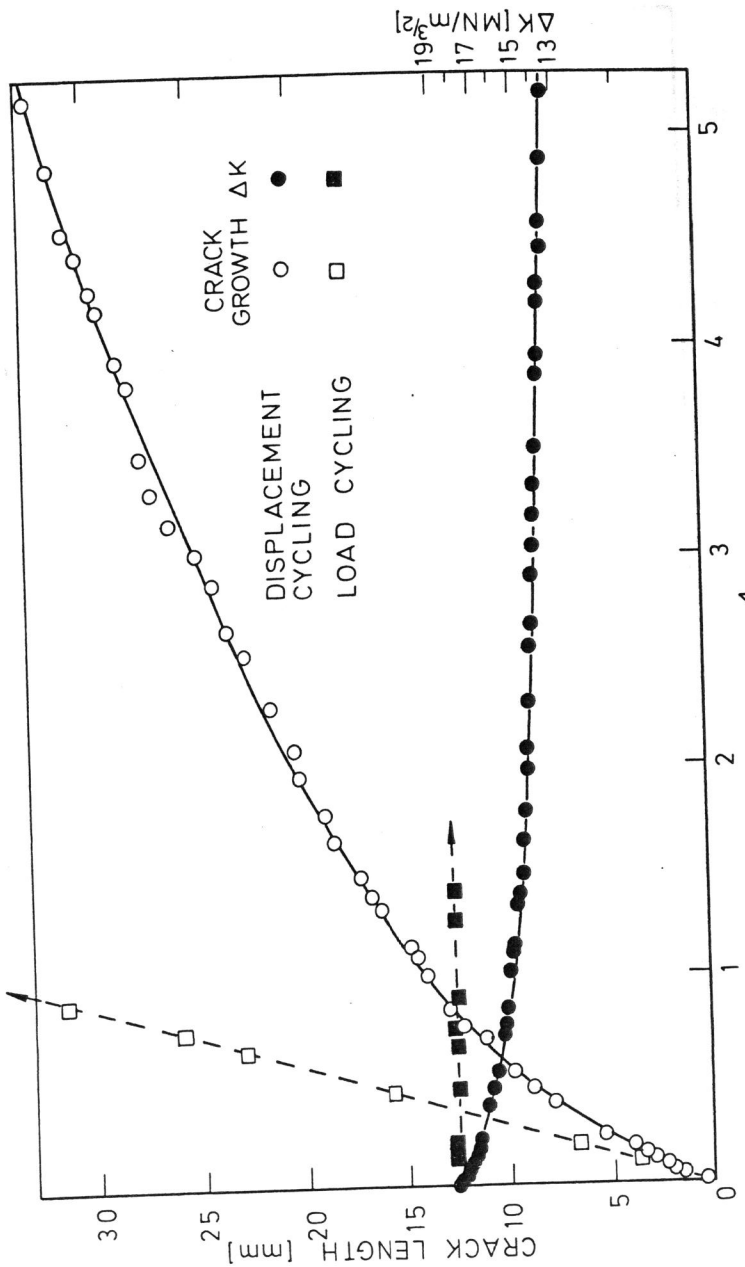

Figure 9: RR58: Fatigue tests, 0.1 Hz and $R \approx 0$

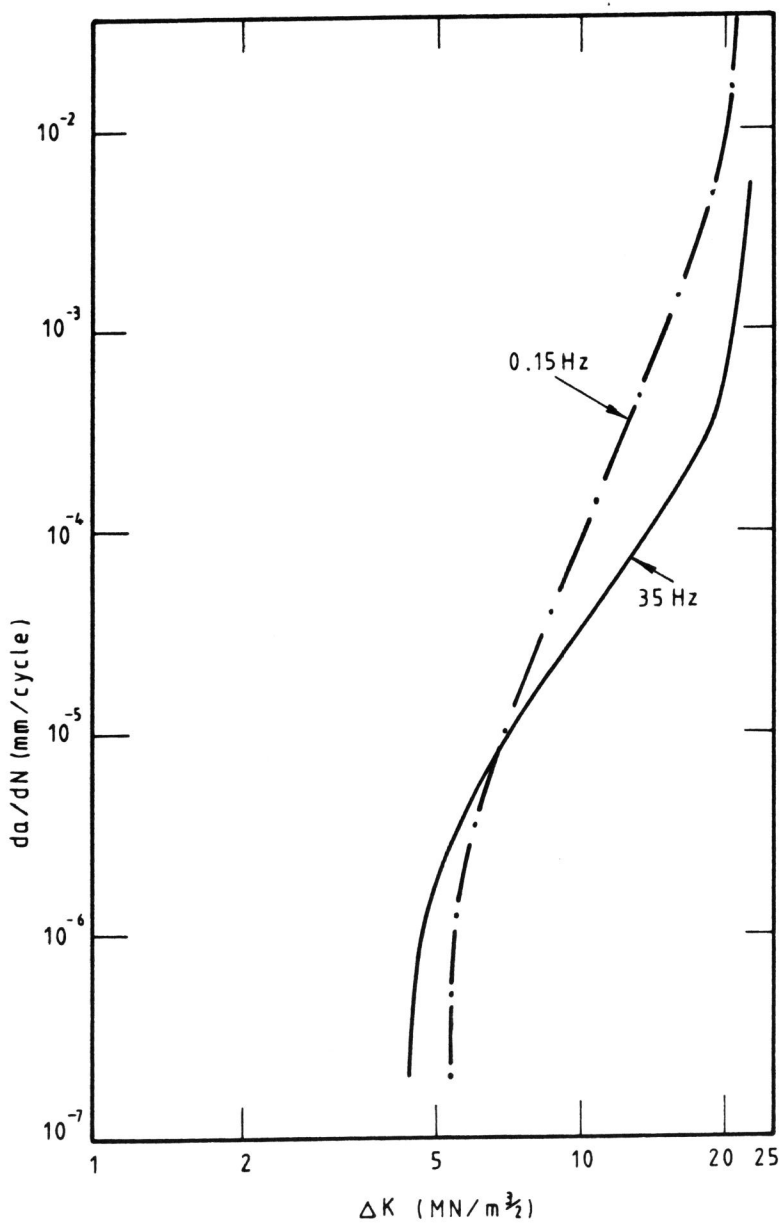

Figure 10: RR58: Crack growth rate versus ΔK. Laboratory air, 0.15 and 35 Hz, $R = 0$